Article

A Comparison of Tidal Turbine Characteristics Obtained from Field and Laboratory Testing

Pál Schmitt [1,2,*] , Song Fu [3], Ian Benson [1,2], Gavin Lavery [3], Stephanie Ordoñez-Sanchez [3] , Carwyn Frost [1,2] , Cameron Johnstone [3] and Louise Kregting [1,2]

1   School of Natural and Built Environment, Queen's University Belfast, Belfast BT9 5AG, UK
2   Queen's University Marine Laboratory, Queen's University Belfast, 12-13 The Strand, Portaferry BT22 1PF, UK
3   Department of Mechanical and Aerospace Engineering, Strathclyde University, Level 8, James Weir Building, 75 Montrose Street, Glasgow G1 1XJ, UK
*   Correspondence: p.schmitt@qub.ac.uk

Abstract: Experimental testing of physical turbines, often at a smaller scale, is an essential tool for engineers to investigate fundamental design parameters such as power output and efficiency. Despite issues with scaling and blockage which are caused by limitations in size and flow velocity of the test facilities, experimental tank testing in laboratory environments is often perceived as offering more control and thus trustworthier results than field testing. This paper presents field tests of a tidal turbine, performed using a self-propelled barge in real tidal flow and still water conditions, that are compared to a towing tank test. Factors influencing the performance characteristics, such as the choice of velocity sensor, vessel handling and data processing techniques are investigated in this paper. Direct comparison with test results of the exact same turbine obtained in an experimental test facility further confirms that field testing with robust data analysis capabilities is a viable, time and cost efficient alternative to characterise tidal turbines.

Keywords: tidal energy; field testing; tank testing; self propelled barge; prototype

1. Introduction

Prototype testing is an important part of tidal stream turbine (TST) development and is usually carried out in laboratories. Laboratory testing however comes with inherent issues including scaling and blockage correction uncertainties as well as inter-laboratory variation. Previous comparisons between laboratories have been undertaken through the European MaRINET and MaRINET 2 projects, where the exact same turbine prototype was tested at different facilities. The first set of Round Robin tests showed that turbines tested with blockage ratios of up to 5% need to be corrected for. In addition, Reynolds numbers differed sufficiently from full scale devices to cause further uncertainty [1]. Wave–current interaction was the main focus of a similar Round Robin test programme [2] undertaken in MaRINET 2. Experiments were replicated with a highly instrumented horizontal axis turbine of 0.72 m in diameter [3]. Irrespective of the testing conditions, similar conclusions could be drawn from the results that the power coefficient differed by an order of 15% to 25% at peak power conditions between tank test facilities. It was also shown that uncertainties in the power performance of a turbine can be as high as 15% between some facilities suggesting the importance of replicating experiments within any testing campaign to improve the reliability of the results.

While laboratory tests can provide similar conditions to real environments, this is often associated with significant costs in time and money. Costs for access to laboratories and charter rates for vessels differ widely, but EUR 5–10k is not uncommon as a day rate for the largest laboratories. Vessels able to tow turbines of comparable size are widely available for approximately EUR 1.5kper day. Towing tanks also require settling time between experiments and typically the carriage must be returned to the end of the tank,

reducing the amount of data that can be obtained to a fraction of the test time, with each run limited to 10 s at best. Testing on a vessel, as described here, allows data to be recorded almost continuously, yielding significantly more data per day.

Few examples of a direct comparison between tank and field testing have actually been published, but many publications discussed below claim that the controlled environment in a laboratory allows for better quality data to be obtained. However, tests in real tidal flows are significant for developers to gain operational experience and might, depending on turbine size, be the only viable option. Field test options include moored or self-propelled short-term experiments. Moored tests are carried out to provide valuable long-term information on high frequency varying inflow over spring/neap tidal cycles in relation to device performance. However, several field investigations have also demonstrated the usefulness of self-propelled short-term experiments.

An early example of a self-propelled short-term experiment of a tidal turbine is the large-scale towing test for Oceanflow Energy's 1:10th scale Evopod model with 1.5 m horizontal axis rotor diameter in Montgomery Lake, Northern Ireland [4]. The test showed that varying the inflow speed (0.9, 1.0 and 1.1 m/s) yielded little difference in the max-imum power coefficients (0.37, 0.33 and 0.35, respectively) and the maxima occurred at approximately the same tip speed ratio (3.2, 3.1 and 3.0, respectively). Ref. [5] performed experiments with a commercial prototype of a full scale turbine of 4m diameter attached to the bow of a tug boat. Complex postprocessing, involving simulations of the flow field around the tug's hull, was required and scatter of the resulting power curves reached up to 25% of the mean values. However, best-fitted curves matched design simulations well and the tests were deemed a success, demonstrating the correct functioning of the control system and passive load shedding capabilities of the blades. SCHOTTEL also carried out self propelled tests in Strangford Lough, Northern Ireland in 2014 with their 4 m rotor diameter Hydrokinetic Turbine prototype [6]. The turbine was tested in steady and unsteady flows by towing it in Strangford Lough with results showing a 5% difference in power performance. Ref. [7] presented power curves of a small scale cross flow turbine towed behind a boat in the field and also used a Vector to measure inflow velocities. The authors concluded specifically that "The method of tow-testing is found effective". Ref. [8] used self-propelled platforms such as landing boats to investigate the performance of a range of ducted, bare helical and straight blade Darrieus hydrokinetic turbines in Canada and Australia. The main issue with those tests was the dependency of turbine efficiency on flow velocity due to low Reynolds numbers. Limitations in platform thrust also reduced the range of achievable inflow for larger turbine models. Another noteworthy prototype test of a non-conventional tidal turbine using a self propelled platform was described by [9]. The power curve obtained had relatively low scatter, with a reported average error of ±2.3%.

When comparing between the laboratory and field, two different horizontal axis turbine rotors (1.5 m diameter) have been experimentally tested at the Institute of Marine Engineering (Istituto di Ingegneria del Mare, INM) and the Queen's University Belfast tidal test centre at Strangford Lough [10,11]. The work focussed on the influence of flow instrumentation and the two main instrument classes available to the industry. Acoustic Profilers, such as Aquadopps, provide spatial information of the flow across the entire depth range, albeit with a sampling frequency of only about 1 Hz. Vectors sample velocity at a single location, but with much higher temporal resolution of 10 s of Hz. The Aquadopp data (in INM) at low carriage velocity showed poor accuracy but were nearly the same as the carriage speed at CNR-INM for higher flow velocities. Strangford Lough Aquadopp data fluctuated between 0.9 and 1.4 m/s during the time series. Authors noted that Doppler noise biasing of the Aquadopp data results in an over-estimate of the inflow power of 1 or 2%, and a corresponding under-estimate of the power coefficient (C_p). The effect on Vector data was found to be negligible for typical field conditions and 1 s averages.

The works described above show some examples of research with the use of self-propelled barges or comparative research between laboratory and real-site testing. There have also been attempts to evaluate tidal stream devices at real sites and compare results

with design tools such as boundary element models. Ref. [12] presented a rare example of full scale turbine power data over several tidal cycles measured in the field in direct comparison with two results from a boundary element model, one using Active Acoustic sensors and another based on a large scale numerical model for flow data. The error between energy production estimates from the numerical model compared with the real output was reported as 7.6% and the energy estimate based on flow measurements resulted in an error of 8.8%.

It can be argued that the aforementioned studies have successfully tested tidal stream turbine prototypes at sea but there are discrepancies between methods which are not well understood. The aim of this work is to improve our understanding of some of these ambiguities by investigating the impacts on power performance based on flow velocity measurements, in a field test with a self-propelled barge and a controlled laboratory setting and compare how these results relate to a boundary element model.

2. Methodology

2.1. Field Setup

All tests were carried out in Strangford Lough using an Easy Worker 1460 anchor handling barge. Length over all, beam and depth at sides was 14 m, 6 m and 1.8 m respectively. The maximum draught was 1.2 m at the aft perpendicular. The barge can achieve 8 knots maximum speed and 4 t maximum thrust under bollard pull conditions. The crane is rated for loads up to 8 t.

The turbine was mounted forward facing below an aluminium truss protruding midship from the bow of the vessel with a hub height of 1.26 m below the water level and at least 10 cm below the bow section, Figures 1 and 2. The vessel was operated in forward speed during all measurements and the influence of the hull on turbine inflow is believed to be negligible.

Flow measurements were performed using two Acoustic Doppler Profilers (Nortek Aquadopp, 2 MHz; Nortek AS, Vangkroken 2, 1351 Rud, Norway) and two Acoustic Doppler Velocimeters (Nortek AS, Vangkroken 2, 1351 Rud, Norway) hereafter referred to as Aquadopp and Vector. The first Vector (V1) measured flow 1.34 m to the portside of the turbine axis and 0.07 m upstream in 0.88 m water depth. The second Vector (V2) was installed downstream, 1.96 m from the turbine plane and at 0.8 m water depth. The first Aquadopp (A1) was mounted 1.24 m starboard and 0.58 m upstream at a depth of 0.45 m. The second Aquadopp (A2) was mounted midship 2.6 m in front of the turbine plane with the sensor head submerged at a depth of 0.45 m with both Aquadopps vertical bin resolution set to 0.1 m. Aquadopps sampled at 1 Hz, Vectors at 16 Hz.

A three-bladed horizontal axis turbine was used for these experiments. The rotor had a diameter of 1.05 m and the blade length was 0.35 m. The blades were designed using a Wortmann FX 63-137 aerofoil profile. The pitch angle was set at 8 deg for all tests. The turbine was equipped with a TorqSense RWT411 torque and rotation sensor and also recorded electrical power with 10 Hz temporal resolution. A sensor at the top of the stanchion recorded turbine thrust with 16 Hz resolution. The Supervisory Control and Data Acquisition (SCADA) system was operated in constant speed mode, attempting to maintain a set-point RPM. The SCADA uses a National Instruments CompactRIO which writes to screen and file allowing for real time monitoring of the inflow and turbine metrics.

All tests were carried out in two different regions of Strangford Lough, Northern Ireland in August 2021. To achieve unsteady, turbulent flows, the barge was first driven in the middle of the Narrows during the ebb tide, details on earlier assessments of the flow conditions there are provided by [13]. A second set of tests was performed in the large bay of Strangford Lough where the water is virtually stagnant and inflow conditions expected to be comparable to towing tank test.

Total water depth was always greater than 20 m to ensure no disturbance by blockage effects. Test runs and data recordings typically lasted 128 s and a total of 105 runs were carried out.
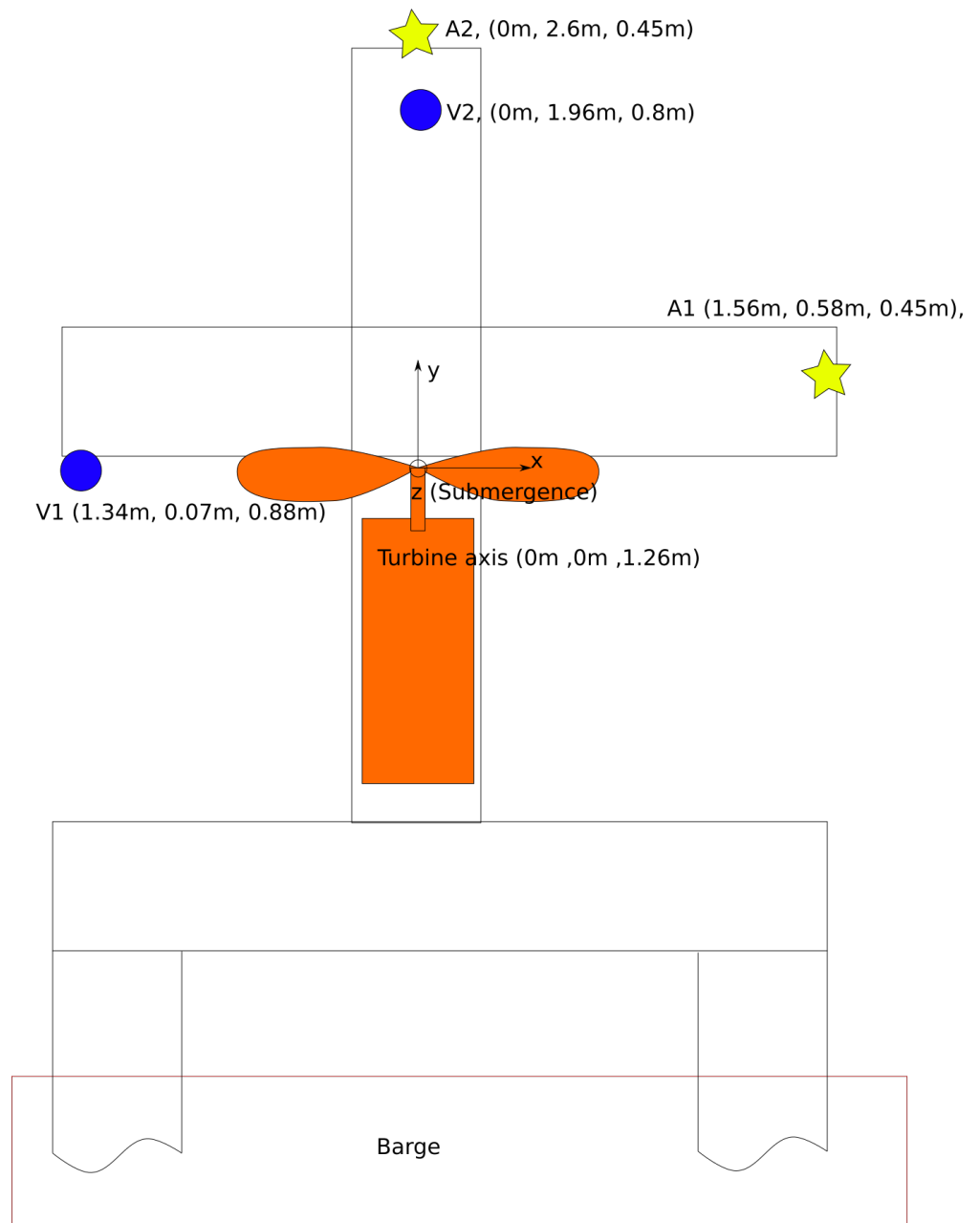
Figure 1. Instrument layout schematic (not to scale). Blue circles show Vector (V) locations, Yellow stars Acoustic Doppler Profilers (A). Distances of the sensor heads from the turbine axis are given in brackets.
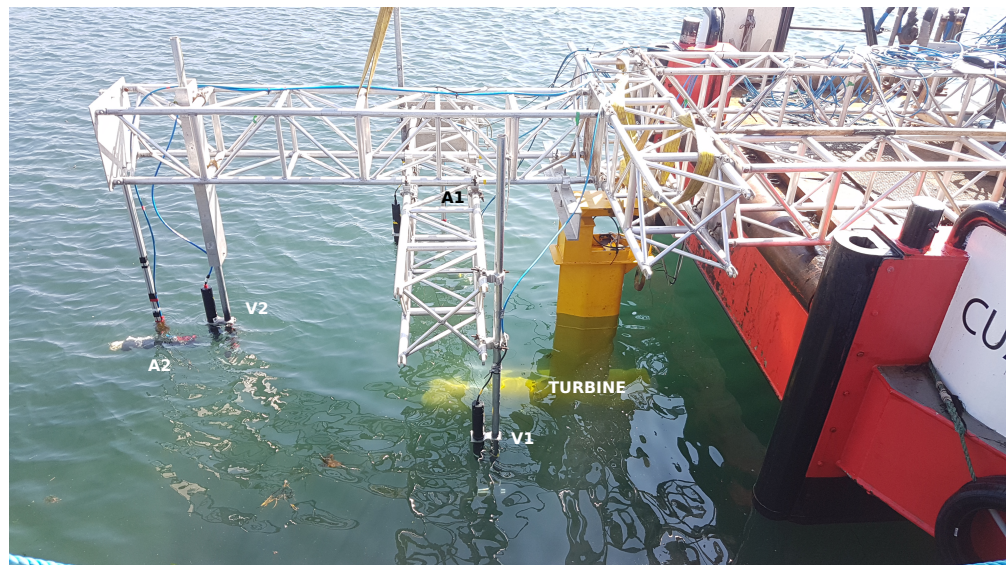
Figure 2. Experimental setup on the barge, seen from shore. Turbine blades are in line with Vector 1 (V1). Aquadopps 1 and 2 are indicated by A1 and A2, Vector 1 and 2 by V1 and V2 respectively.

2.2. Tank Setup

To compare the field tests with controlled laboratory testing, experiments were also undertaken in a tow tank located at Kelvin Hydrodynamic laboratory (KHL) at Strathclyde University, Glasgow, UK. The turbine setup can be seen in Figure 3. Table 1 shows the characteristics of the facility and the settings used for the laboratory tests. The Reynolds number calculation is based on [1]. Data from tank tests relied on carriage speed for turbine inflow velocity.
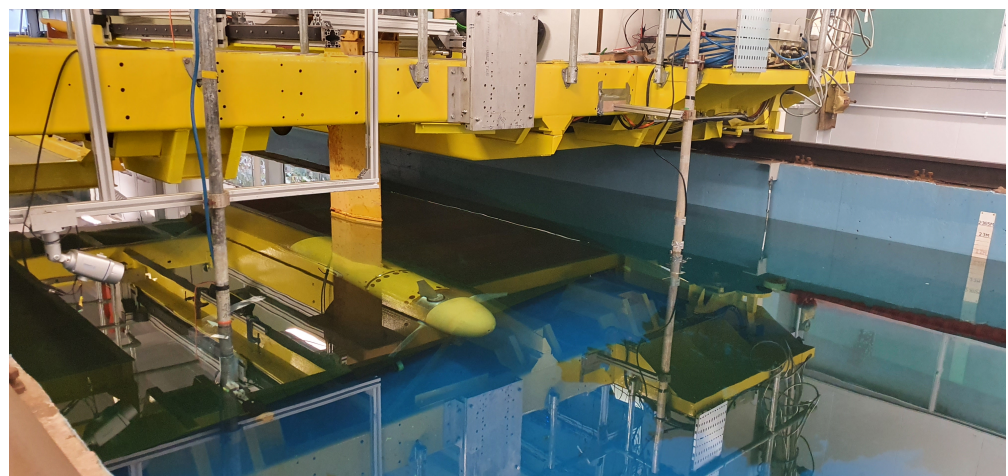

Figure 3. Turbine installed at the Kelvin Hydrodynamics Laboratory.

Table 1. Kelvin Hydrodynamics Laboratory specifications.

Parameter	Value
length $\times$ width $\times$ depth	76 m $\times$ 4.6 m $\times$ 2.5 m
Flow velocity	Maximum speed 5 m/s
Blockage ratio	6.97%
Flow velocities tested	1.7, 1.8 and 2.0 m/s
Repeated tests per flow speed	2, 2 and 3
Number of data sets per flow speed	24, 32 and 54
Reynolds number at 70% of the blade length at $\lambda = 4$ per flow speed	5.16×10^5, 5.46×10^5 and 6.07×10^5

The turbine was installed to the carriage using steel frames mounted to the carriage structure, as can be observed in Figure 4. The flow velocities tested with the tow carriage were based on real-site trials. However, during the test at KHL, at low flow velocities, the turbine only started operating after the mid-section of the tow tank, yielding few useful data. Thus, the laboratory campaign focused on the evaluation of the three higher velocities listed in Table 1 for which repeated tests were carried out.
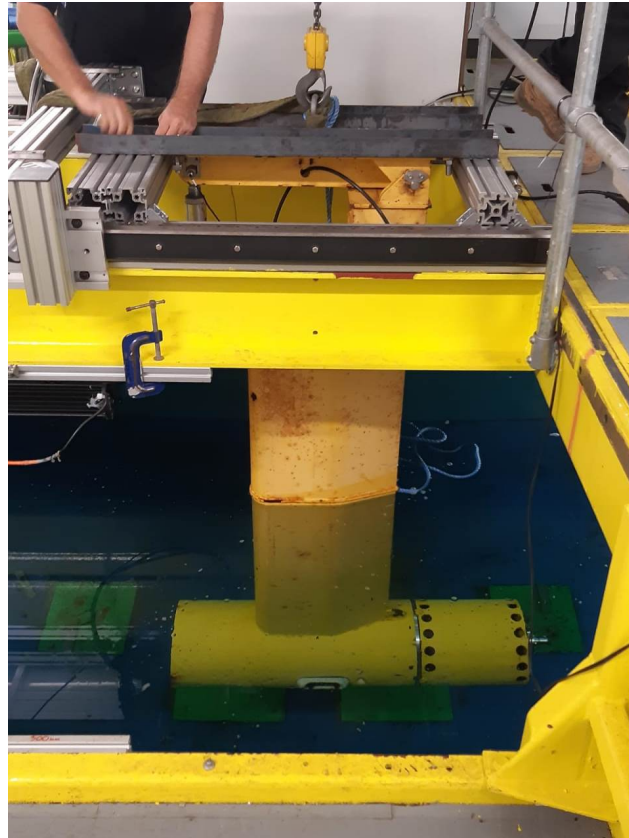

Figure 4. Mounting frames used to support the turbine to the main carriage.

As observed in Table 1, the blockage ratio within the tow tank facility was 6.97% which requires blockage correction of the experimental data. We followed the methods presented by [14,15]. Thrust force was available from the turbine sensors.

2.3. Vector Processing

Data from the Vector probes u was filtered by employing a Phase-Space Threshold Filter (PST), following the methods described by [16]. Filtered data are indicated by the index f.

A steadiness parameter α was established by evaluating the slope of the linear best fit line for each 30 s window along the entire dataset. The overlap of the windows was 5 s. The section with the lowest absolute α value was selected for further processing and is indicated by the index s. Figure A1 shows an example data trace, the best fit line segments and the selected sections with the lowest α value. Figure A2 shows an example time trace of the raw, filtered and steadiest Vector data section.

The mean value $\bar{u}_f$ of the selected 30 s section was saved for each direction and the inflow angle evaluated as

$$\theta = asin(\frac{\bar{u}_{y,s}}{\bar{u}_{x,s}}) \tag{1}$$

Turbulent kinetic energy (k) was approximated from Vector data as

$$k = 0.5(Var(u_{x,f,s}) + Var(u_{y,f,s}) + Var(u_{z,f,s})) \tag{2}$$

with *Var* being the variance.

2.4. Aquadopp Processing

Depth averaged (DA) mean values of the entire time trace for raw and filtered data and the section corresponding to the steadiest flow according to the Vector data were obtained for further processing. Initially, the Aquadopp data were filtered (index $_f$) by applying a single pass replacement of any velocity values corresponding to response amplitude counts below 50 with the mean of the closest neighbouring values in time and space. Figures A3–A6 show raw and filtered velocity data in x direction over time and bin number for A1 and A2. In addition, two scalar values were determined for the time trace corresponding to the steadiest section, based on the analysis of V1:

- The parameter γ was obtained as the slope of the linear best fit over the mean x velocity values at each depth bin to assess the vertical flow profile.
- The parameter δ was evaluated as the mean root square of the DA velocities in x direction to assess the temporal variation around the mean.

Figure A2 shows raw and filtered depth-averaged data beside the Vector data as discussed above.

2.5. Turbine Data

The power of the turbine was analysed based on the following non-dimensional parameters of Tip Speed Ratio λ and Coefficient of Power C_p.

Tip Speed Ratio λ was evaluated as

$$\lambda = \frac{r\omega}{u} \tag{3}$$

with r the turbine radius of 0.525 m, and u was based on the data from each instrument or the carriage velocity.

The Coefficient of Power was obtained as

$$C_p = \frac{P}{P_{inflow}} \tag{4}$$

with $P_{inflow} = \rho r^2 \pi u^3/2$ and P either electric power P_E recorded directly by the DAQ or mechanical power P_M evaluated from torque T and rotational velocity ω as $P_M = T\omega$. ρ is the fluid density and was set to 1025 kg/m^3. Similar to the treatment of velocity data, power and rotational speed values were either the mean of the entire trace or corresponding to the selected steadiest section.

2.6. Blade Element Model

The turbine blades used in this work were designed using an in-house blade element momentum theory (BEMT) model [17,18] and outputs are also shown for comparison with tank and field results. Details on the method and validation cases can be found in [15,19,20].

3. Results and Discussion

Figure 5 presents $C_p - \lambda$ data from all test runs using the mean of the complete unfiltered and DAV data for each run and mechanical or electrical power. All C_p values start at λ of 1 and maximum power is achieved around a λ of 3. Mechanical power is consistently 30% higher than electrical power. Up to a λ of 3, data evaluated using the Vector compare well to the Aquadopp data and show little scatter. For λ values above 3, scatter increases and Vector data consistently predict higher power values than the Aquadopps. Overall, this analysis without further data selection or filtering already provides a clear

understanding of the turbine characteristics. In the following sections, the influence of different filters and data selection strategies will be investigated.
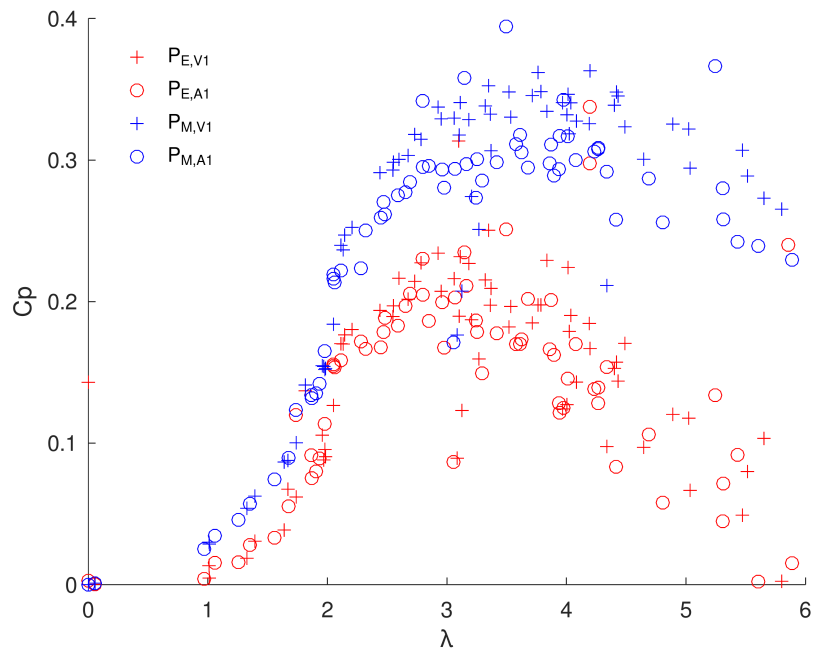

Figure 5. C_p–λ data for all runs performed in the field, with no filtering applied. Power is based on electrical (P_E) or mechanical (P_M) data, inflow is measured using mean x velocity u for the Vector 1 or depth averaged velocity (DAV) data over all bins for the Aquadopp 1.

As flow dynamics in the field are much more variable in the field than in the lab, for example due to vessel handling, waves from passing boats or large scale flow patterns, data were limited to the steadiest condition with similar duration as the laboratory tests. Figure 6 shows $C_p - \lambda$ data obtained using raw and the steadiest, filtered 30 s section for V1. Scatter is reduced considerably for λ above 3 while maintaining excellent agreement for the lower λ values.
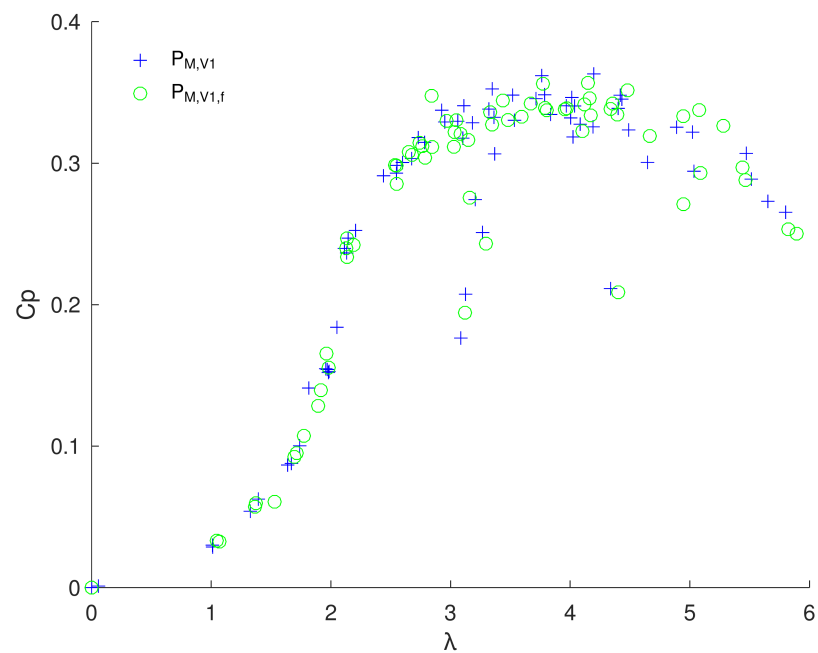

Figure 6. C_p–λ data based on mechanical power and Vector1 raw data ($P_{M.V1}$) vs steadiest 30 s sample ($P_{M.V1,f}$).

It could be argued that choosing the steadiest section of each run might still include data where flow acceleration is large and thus affecting turbine characterisation. Figure 7 presents the same V1 data coloured by the steadiness parameter α. The range of α is very small with values ranging between ± 0.04, and most values in the range of ± 0.02. No obvious trend appears with highest and lowest values of α yielding results in line with each other and indicating that this simple data selection procedure is sufficient to obtain useful data sets.

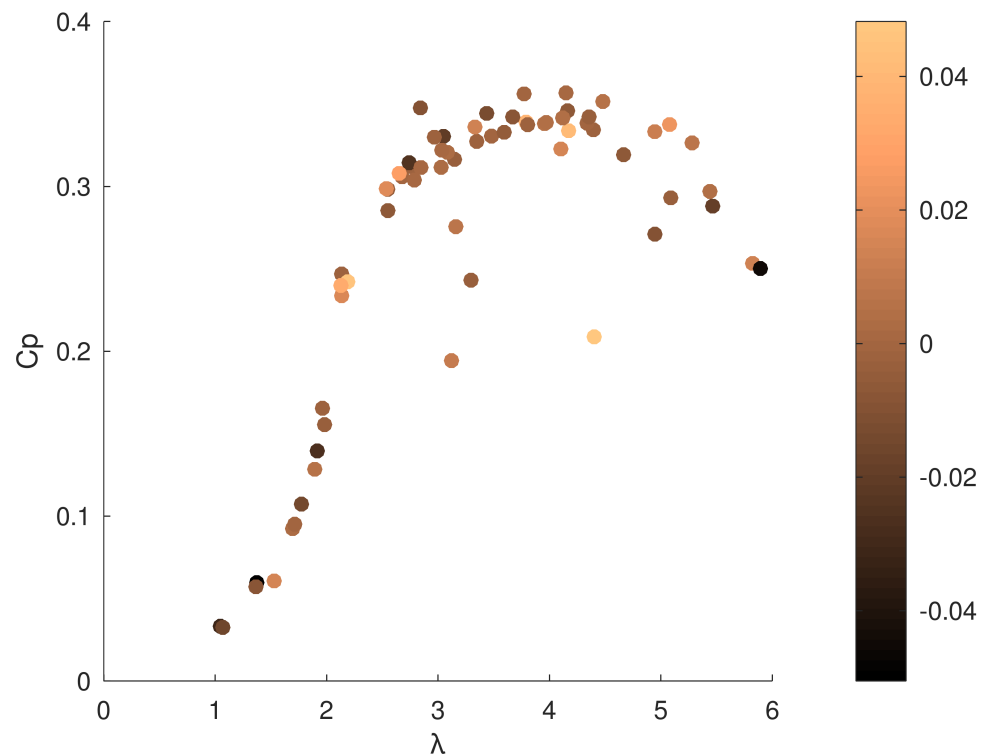**Figure 7.** C_p–λ data based on filtered steadiest 30 s samples from V1. Coloured by steadiness parameter α.

In laboratory tank tests blockage causes flow acceleration around the turbine such that velocity must be measured some distance upstream or separate tests must be run without the turbine present. Figure 8 shows filtered data from V1 and V2. Again agreement is good below a λ of 3. However, above a λ of 3, V2 data exhibits a larger scatter, with C_p values ranging between 0.24–0.32. In contrast, V1 describes almost a flat plateau at 0.32 for λ between 3 and 4.5. The reason for this difference is not clear and requires further investigation. It is possible that the time lag between flow velocity at the position of V2 and the turbine might be a contributing factor. Therefore, in the following section we focus on the Vector probe in line with the turbine, V1.

During the experimental runs, the skipper could only visually estimate flow direction from surface features but not monitor the flow measurements. Figure 9 shows data from V1 coloured by flow angle magnitude. The maximum flow angle of all data sets is only 5 deg, indicating excellent manoeuvring of the barge. There is no obvious recognisable trend between inflow angle and data scatter, with maximum and minimum flow angles yielding almost identical results. Data points which are seemingly outliers like the highest C_p value at λ 3 were obtained at an inflow angle of less than 1.5 deg. This result is in-line with previous research related to flow directionality (yaw angles) in tidal turbines [21].
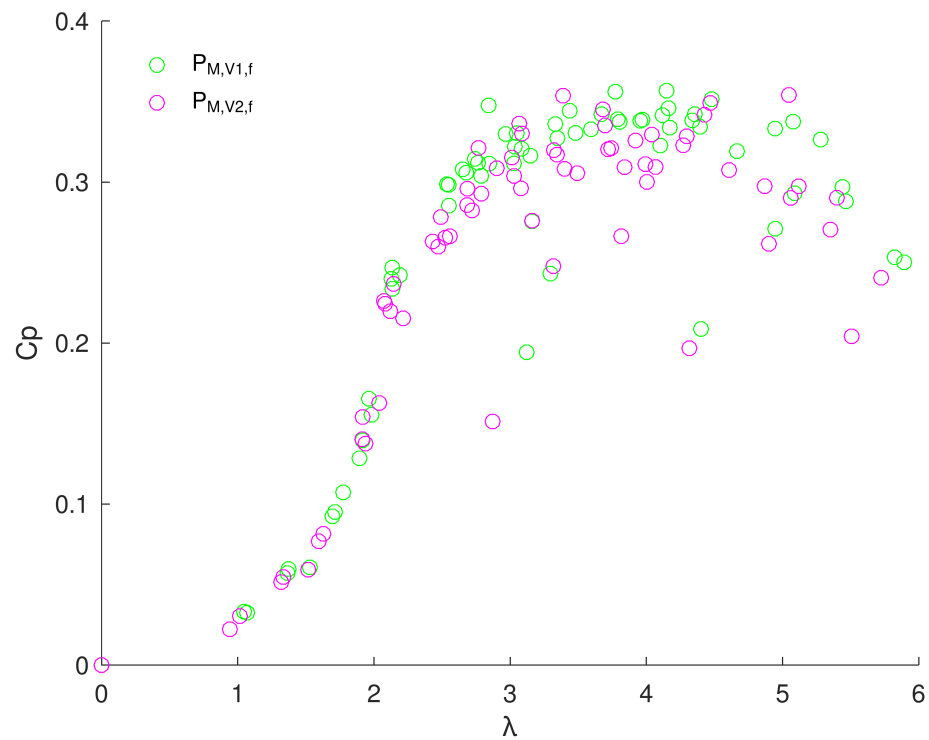
Figure 8. C_p–λ data based on of filtered Vector 1 vs Vector 2 data.

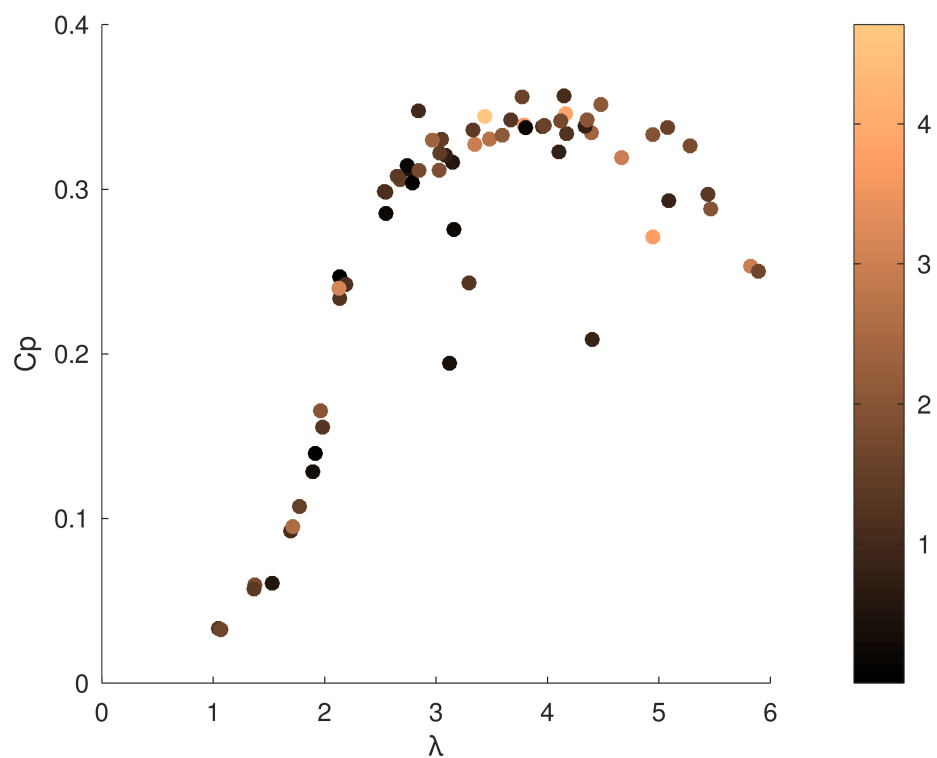**Figure 9.** C_p–λ data based on filtered steadiest 30s samples from V1. Coloured by absolute inflow angle in degrees.

The turbine was operated using a constant RPM. It might have been expected that mean flow velocity and the associated variations of turbine loading influence efficiency. Remarkably, as shown in Figure 10, runs performed at the lowest and highest velocities yielded excellent agreement around the peak C_p values of 0.3 at λ 3 to 4.
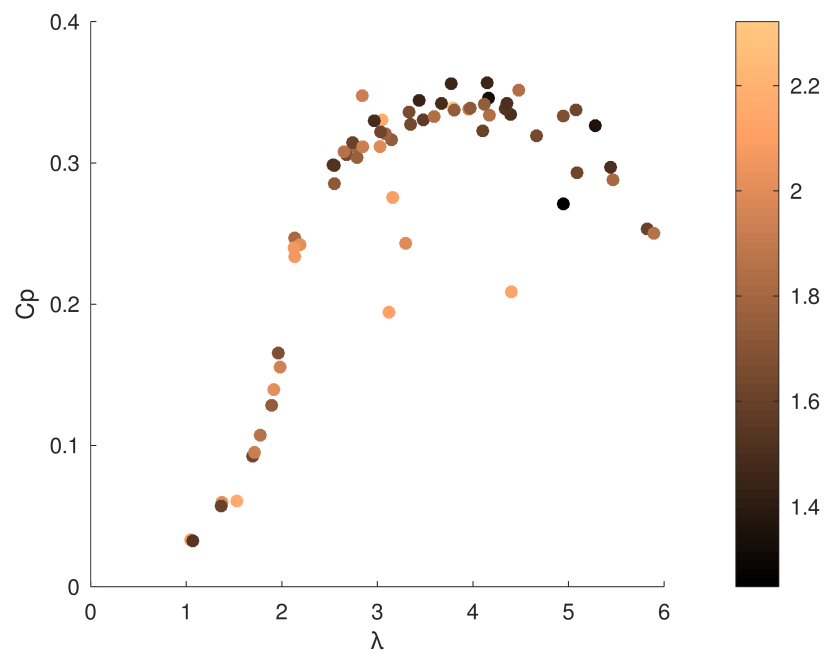
Figure 10. C_p–λ data based on filtered steadiest 30 s samples from V1. Coloured by mean velocity (m/s).

The assessment of turbulence levels in tidal flows and their effect on tidal turbines is still a very active area of research. The wide basin of Strangford Lough with practically standing water is a very different environment from the highly energetic flow in the Narrows channel.

Figure 11 presents data split by test location, Narrows or Lough. Resulting C_p–λ curves are similar overall. The four clear outliers in the data, three for $\lambda = 3$ and a further for 4.5, were all measured in the Lough.
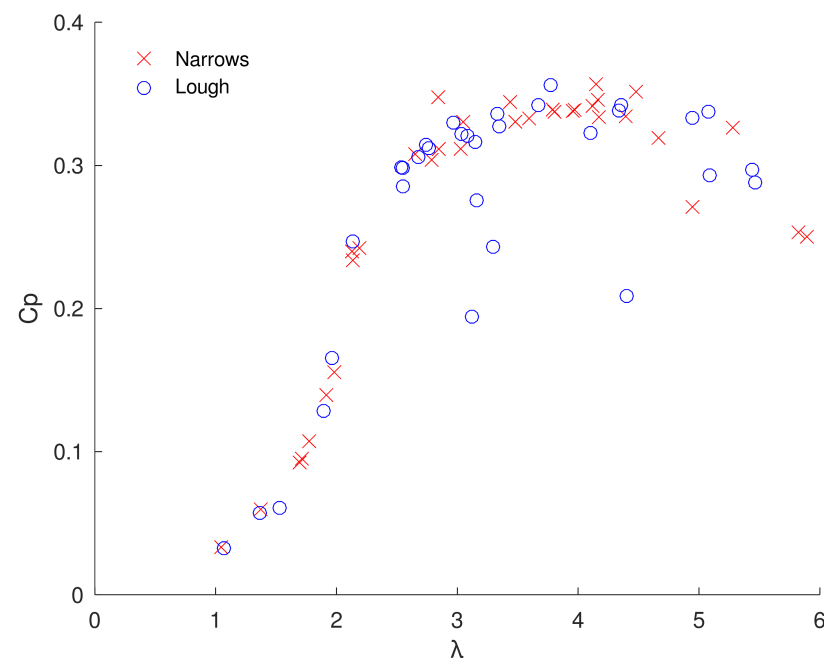

Figure 11. C_p–λ data based on filtered steadiest 30 s samples from V1, classified by location, Narrows (energetic) or Lough (still water).

Similarly, turbulent kinetic energy levels encountered during testing do not seem to influence C_p values either, Figure 12, with values evenly distributed across the entire λ range and outliers not showing a clear correlation with extreme values of k. As expected, the four most extreme outliers, which as discussed above were measured in the Lough, show very low turbulence levels. Comparison with Figure 11 also reveals that the highest turbulence levels, for example the highest C_p value at $\lambda = 4$ and the data for $\lambda = 5.8$ were obtained in the Narrows. These specific results are of course very much turbine dependent, but they highlight the ease with which turbines can be tested at different turbulence levels in the field.
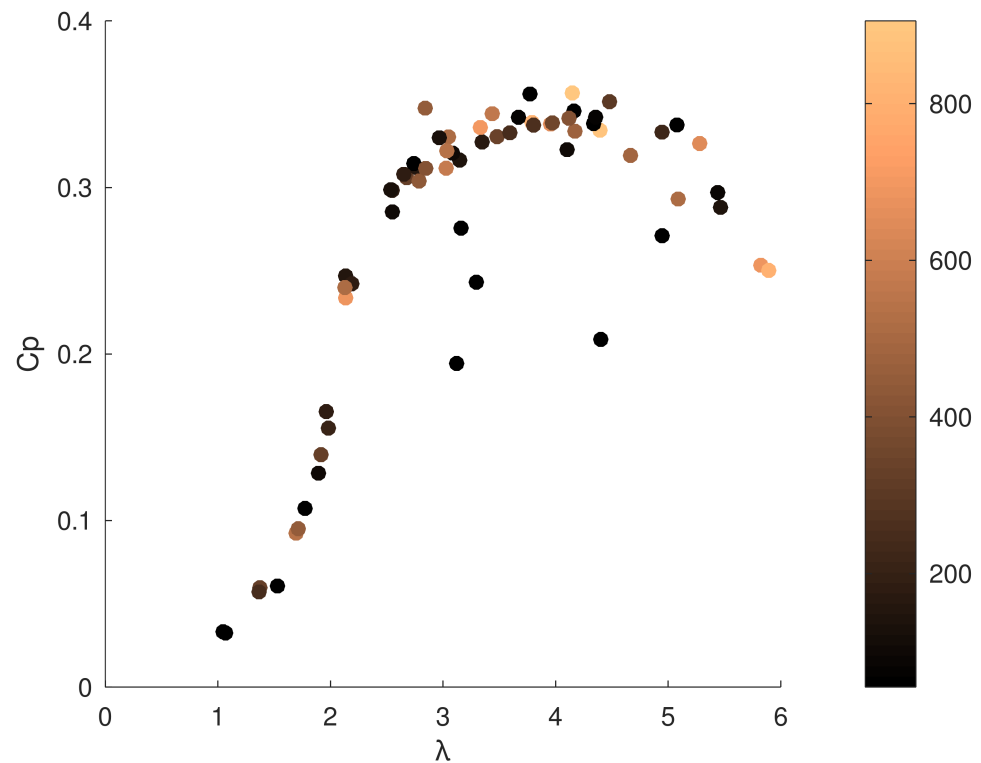

Figure 12. C_p–λ data based on steadiest 30 s sampled from Vector 1, coloured by k.

Acoustic Doppler Profilers can provide information across the water column, albeit with much lover temporal resolution than Velocimeters. Figure 13 shows the mean flow velocity values of DA, filtered DA, entire bin 5 and steadiest 30 s sections according to V1 data. The flow velocities range from -1.5 to -2.5 m/s with the majority of the data between -1.7 and -2.2 m/s. Filtering has no noticeable effect on DA data. The single bin data over the entire time trace generally also agree well with the DA values. For runs 20–30 single bin data tend to yield 0.01 m/s higher flow speeds. However, even if DA and single beam data agree, the selected steadiest 30 s sections can show differences of up to 0.2 m/s, for example for run 21.

Figure 14 shows a direct comparison of resulting C_p–λ data obtained using DA filtered data from both Aquqadopps and data corresponding to the steadiest 30s section according to V1. Overall agreement between A1 and A2 is very good. All processing methods yield almost identical results for λ below 2.5. Higher λ values shows some outliers for DA data, the two most prominent from A1 at λ 3.5 and 5.3.
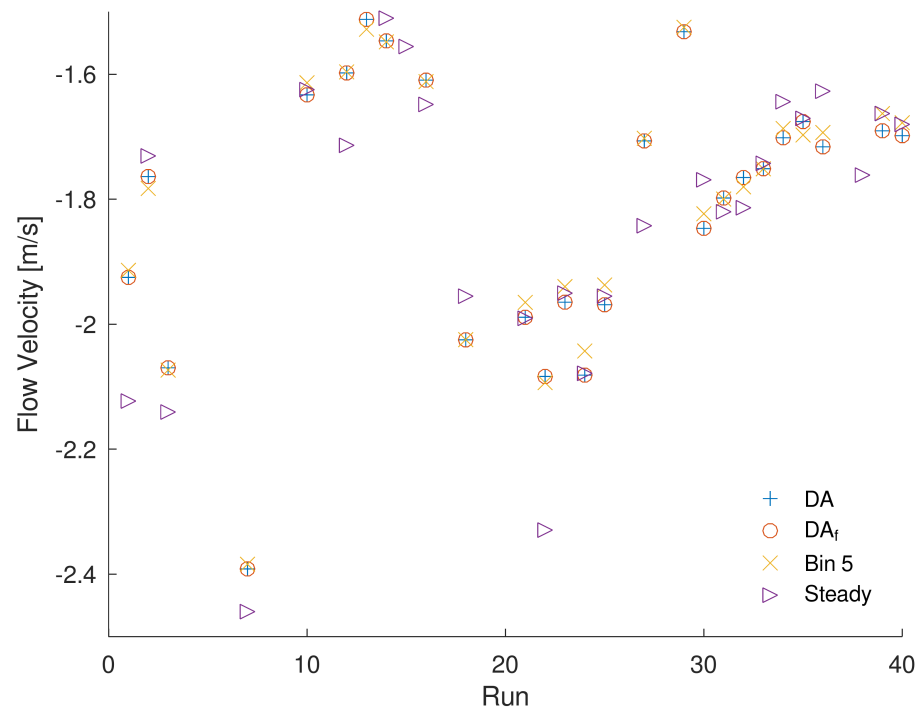
Figure 13. Comparison of raw depth–averaged data (*DA*) from Aquqadopp 1 from the entire timetrace, compared to filtered data (*DA_f*), data from only a single bin (*Bin* 5) and the depth–averaged values obtained from the steadiest 30 s section (*Steady*) according to Vector 1.
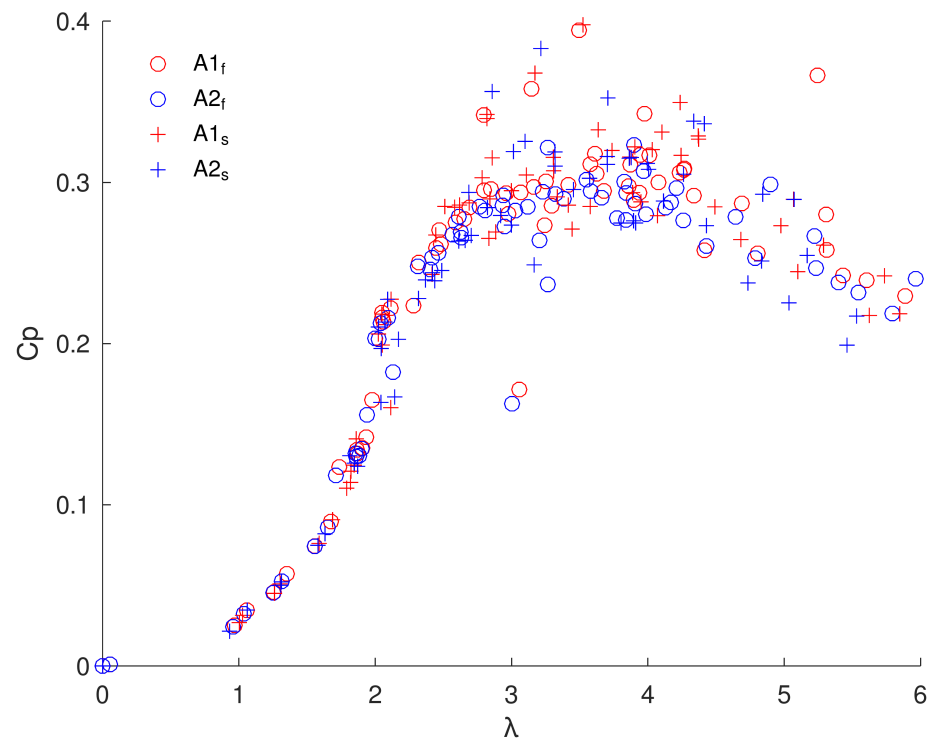

Figure 14. C_p–λ data based on filtered DA and steady A1 data vs A2 data.

Figure 15 shows DA, single bin and steadiest section A1 data coloured by γ. Slope values range from 0.03 to −0.07. Almost all runs resulted in negative slopes. Varying C_p values for a given λ did not differ in slope, for example at λ 3 or 4.5, C_p values range from 0.23 to 0.32.

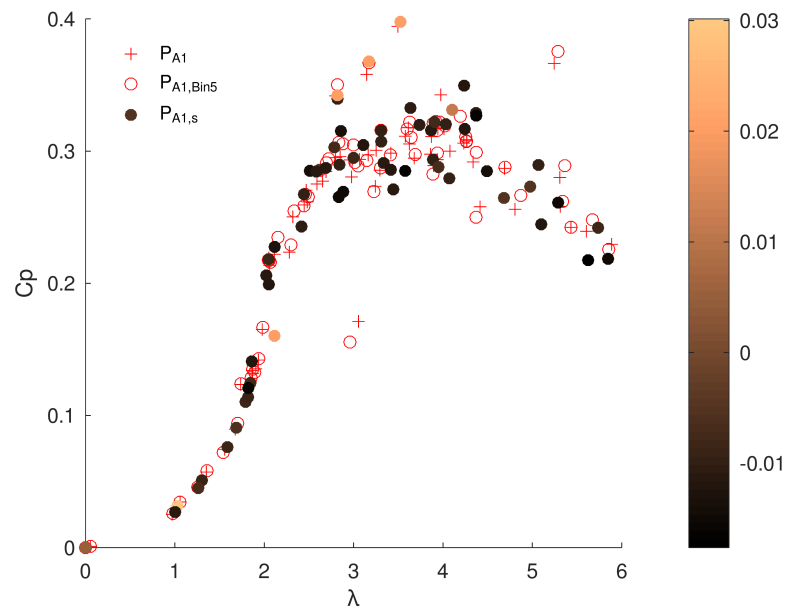**Figure 15.** C_p–λ data based on raw DA A1 data vs selected bin 5 vs steady 30 s section according to V1. Colour indicates vertical slope.

Similarly the δ parameter shows no clear trend or extreme values but minimum and maximum values occur in close proximity, Figure 16. Due to the great water depth and relatively small turbine diameter, the inflow in these experiments was not affected by a shear or wave profile as will typically be the case for larger turbine prototypes installed on the sea floor or in surface proximity. The results indicate overall good agreement between Profilers and Velocimeters and confirm the common practice of using a combination of these sensors to obtain spatial and temporal flow information.
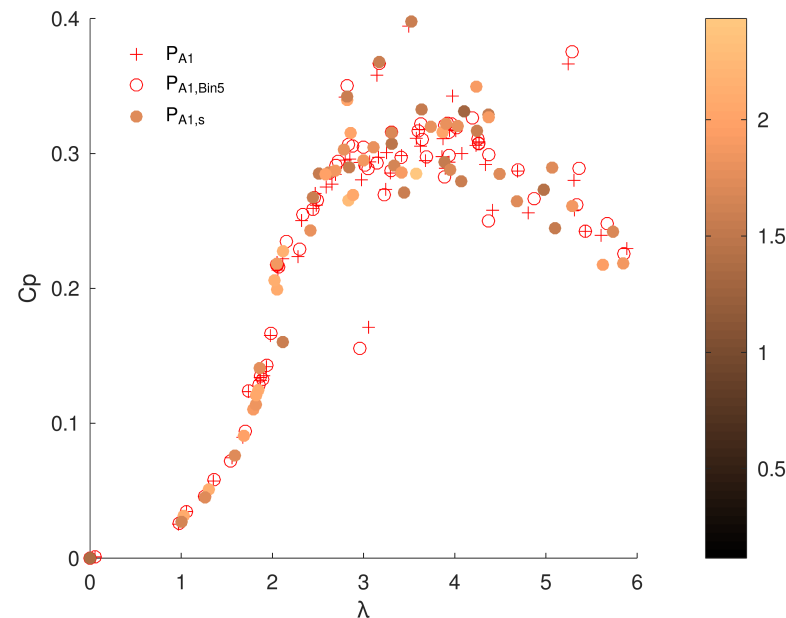

Figure 16. C_p–λ data based on raw DA A1 data vs selected bin 5 vs steady 30 s section according to Vector 1. Colour indicates rms (Ux,steady across bins)

Comparison with Tank and Numerical Data

Figure 17 shows C_p–λ data from field (V1$_{f,s}$) and tank data (Tank) as scatter diagrams. Lines were fitted as piecewise cubic splines to those points using the GNUoctave splinefit

function and are shown as curves Fit_{V1} and Fit_{Tank} repectively. Furthermore, blockage correction was applied to the tank data and the result is shown as $Fit_{Tank,BC}$. Data from the numerical model is shown as a dashed black line labeled BEM.
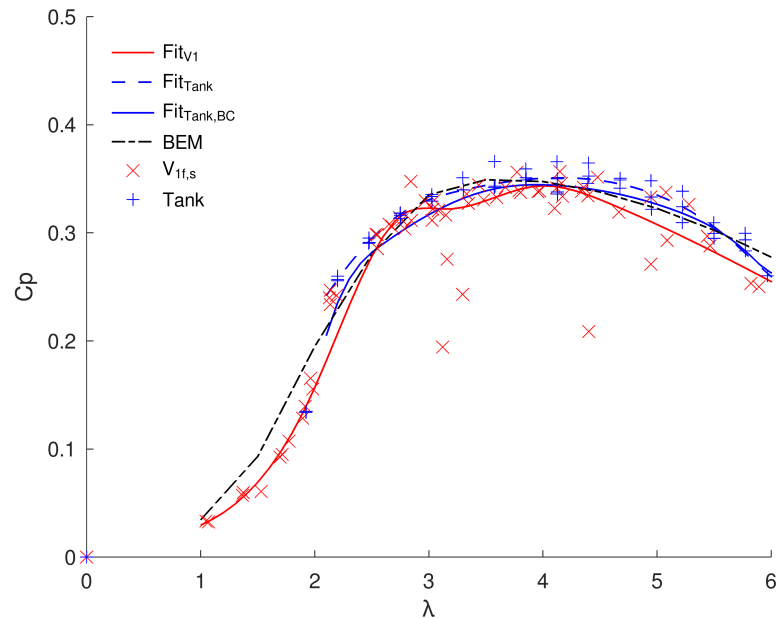

Figure 17. C_p–λ curve obtained from field V1, filt and tank data. Lines were fitted as piecewise cubic splines using the GNUoctave splinefit function. Constraints are set to force the position (2, 0.124).

Raw data show a trend of higher C_P values for tank data and the best fit line yields a maximum value of 0.354 for $\lambda = 4$, somewhat above the best fit line from the field data which yields $C_P = 0.344$. Blockage correction results in an almost perfect match between tank and field data for λ in the range of 3.5 to 4.5. BEM data also agree very well in this range. Across lower and higher λ values agreement is still very good, with maximum deviations between field and blockage corrected tank data of less than 1% C_P.

4. Conclusions and Future Work

A three-bladed horizontal axis turbine prototype was tested at Strangford Lough and a tow tank facility at Strathclyde University. The aim of the Marinet2 testing programme was to investigate the effects on power performance when a turbine operates in real seas using a self-propelled barge and in still water conditions (laboratory facility). The main findings are described as follows:

- Overall, the agreement between the field and tank data for this particular turbine was found to be very good once the blockage correction was applied. In addition, the results are further validated by the good agreement with the BEM design method.
- Without advanced postprocessing or filtering of the data, the quality of the data was good enough to obtain reasonable C_p–λ curves using either the Vector or Aquadopp data.
- Applying standard PST filters and selecting steady 30 s sections significantly reduces scatter for Vector data. In addition, the steadiest sections extracted from each run showed very low levels of flow acceleration/deceleration and no influence on C_P could be found for the levels encountered.
- C_P values evaluated using the upstream Vector resulted in a larger scatter than the inline probe.
- Aquadopp yields a larger scatter than Vector based data, even when the flow is not affected by vertical shear.
- Inflow angles were generally less than 3 deg and never higher than 5 deg. Data revealed no trend between inflow angle and C_P values, confirming previous work that inflow angles below 5 deg are acceptable.

- Mean flow velocity, mean rotational velocity of the turbine, test location in tidal channel or still water, or turbulent kinetic energy had also no discernible influence on C_p data scatter. While these results can be expected to be largely turbine dependent, they emphasise that results were obtained for a larger range of conditions than is viable in most tank tests and indicate the robustness of the presented approach.

While this initial test has yielded promising first results, future work and refinements to the use of self propelled barges is still required. A key limitation is the vessel speed–thrust characteristic, which, as in towing tanks, will limit the maximum turbine size. Testing of wave current interaction effects will also require more complex data acquisition and postprocessing to compensate for platform motion and is an area we hope to develop in the future.

Author Contributions: Conceptualization, P.S., I.B., G.L., S.O.-S., C.F., C.J. and L.K.; Data curation, P.S. and S.F.; Formal analysis, P.S.; Funding acquisition, C.J. and L.K.; Investigation, P.S., S.F., I.B., G.L., C.F. and L.K.; Methodology, P.S., I.B., G.L., S.O.-S., C.F. and C.J.; Project administration, P.S., G.L., S.O.-S., C.J. and L.K.; Resources, I.B.; Software, P.S. and S.F.; Supervision, P.S., S.O.-S. and C.J.; Validation, P.S.; Visualization, S.F.; Writing – original draft, P.S., S.F., I.B., S.O.-S., C.F., C.J. and L.K. All authors have read and agreed to the published version of the manuscript.

Institutional Review Board Statement: The views and opinions expressed in this paper do not necessarily reflect those of the European Commission or the Special EU Programmes Body (SEUPB).

Informed Consent Statement: Not applicable.

Data Availability Statement: The data presented in this study are available on request from the corresponding author.

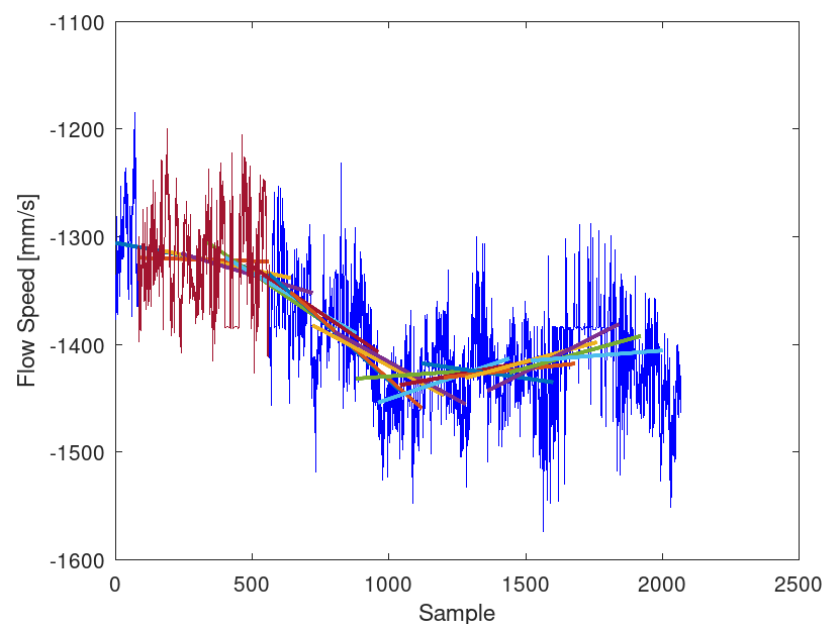**Conflicts of Interest:** The authors declare no conflict of interest.

Appendix A

Figure A1. Example of Vector data processing. Lines indicate best fit straight lines over 30 s, slope is used as steadiness parameter. Steadiest section selected for evaluating power curve is coloured in red.
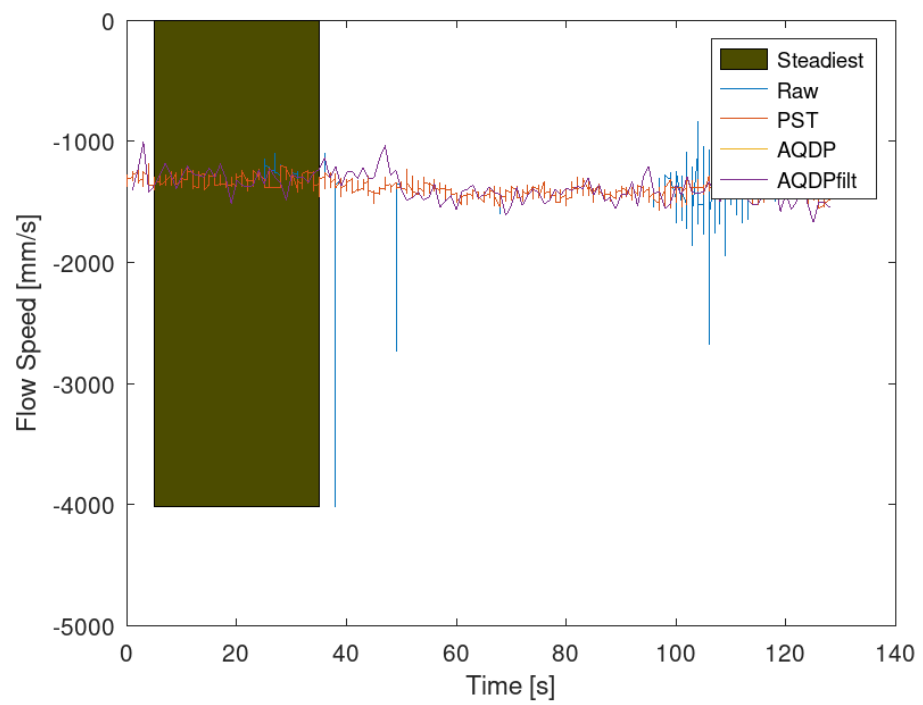
Figure A2. Example of an inflow data set. Raw and PST filtered Vector data. The selected steadiest 30 s section is highlighted. Raw and filtered Depth averaged flow velocity from Aquadopp sensor is also shown.
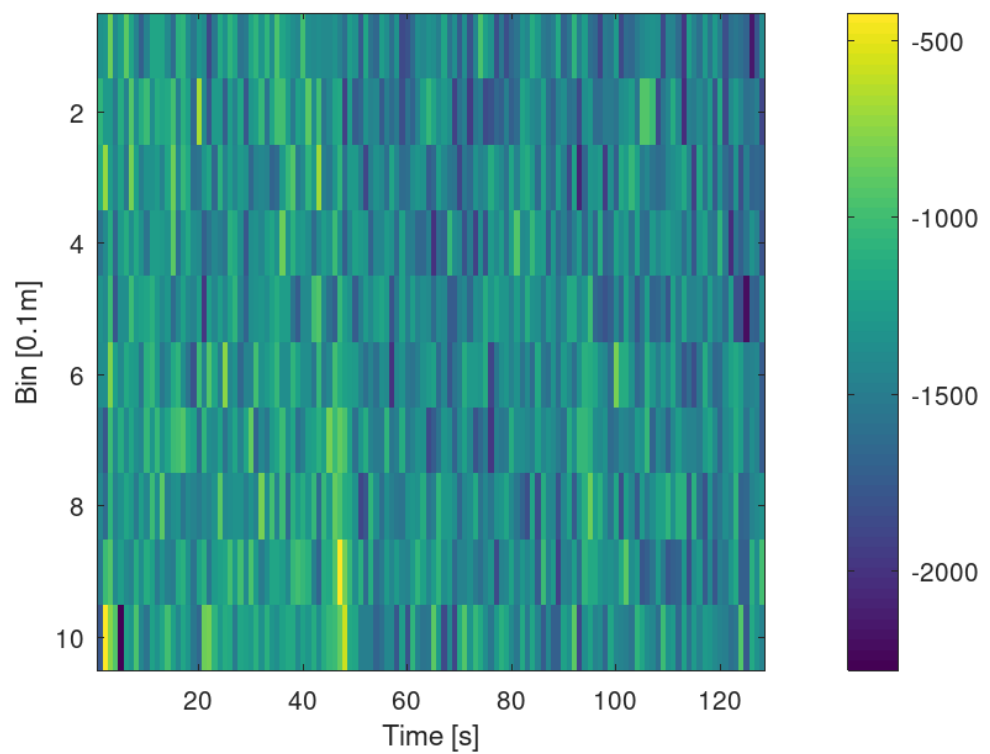

Figure A3. Waterfall plot of inflow x–velocity for Aquadopp1 in mm/s. Bin size is 0.1 m.
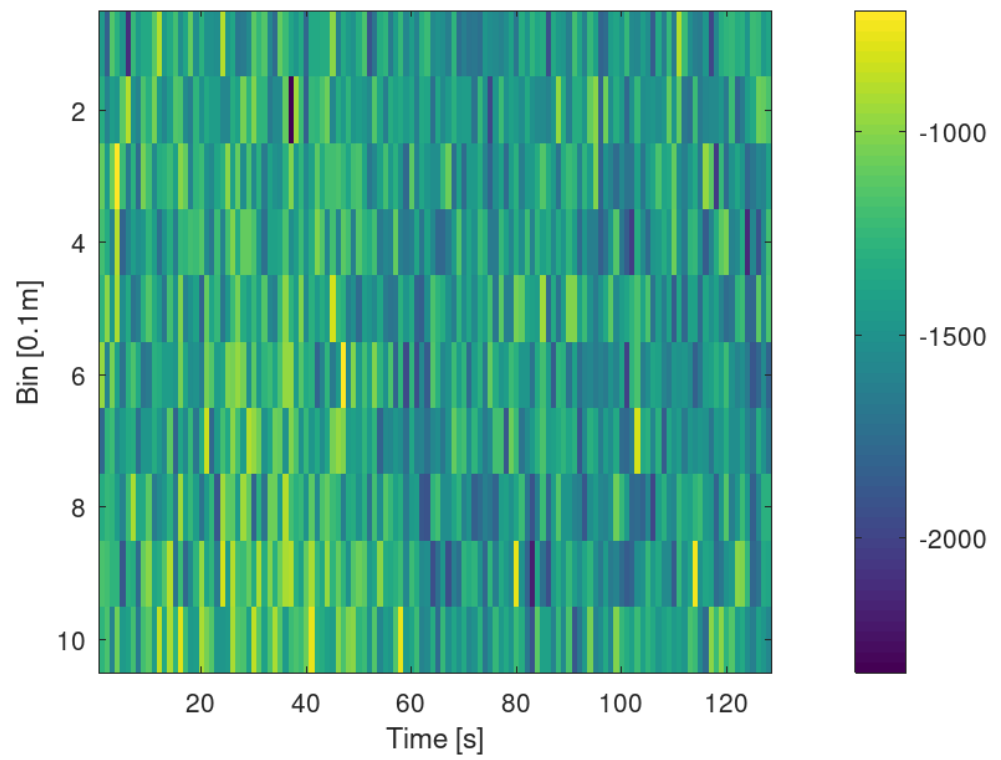
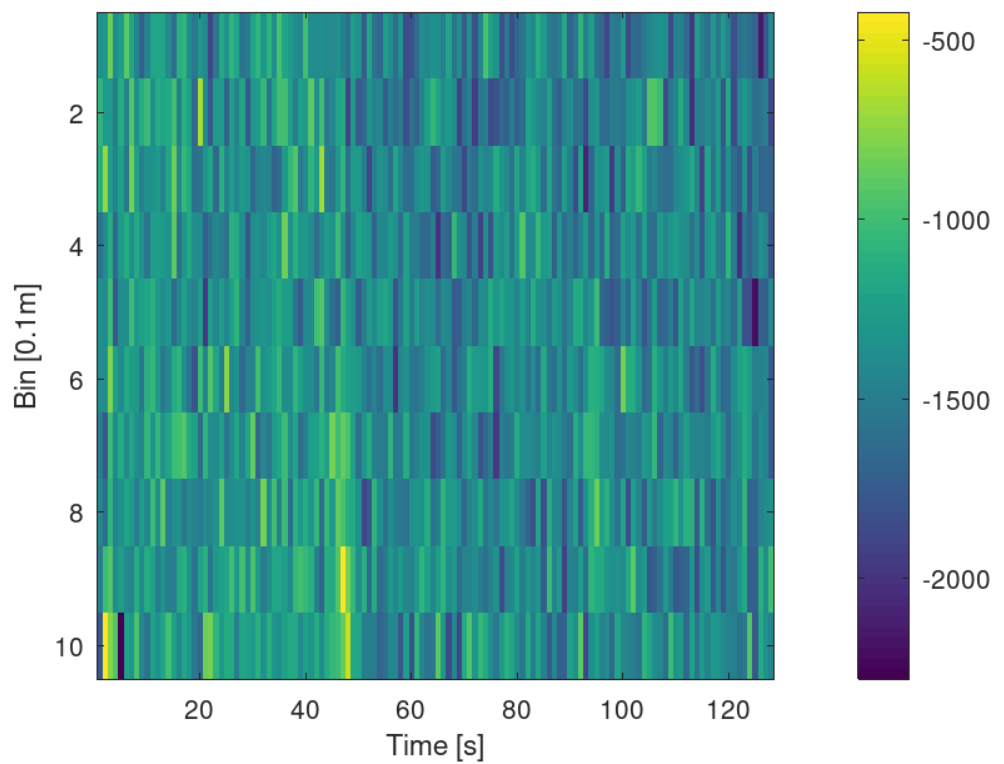**Figure A4.** Waterfall plot of inflow x–velocity for Aquadopp 2 in mm/s. Bin size is 0.1 m.

Figure A5. Waterfall plot of filtered inflow x–velocity for Aquadopp 1 in mm/s. Bin size is 0.1 m.
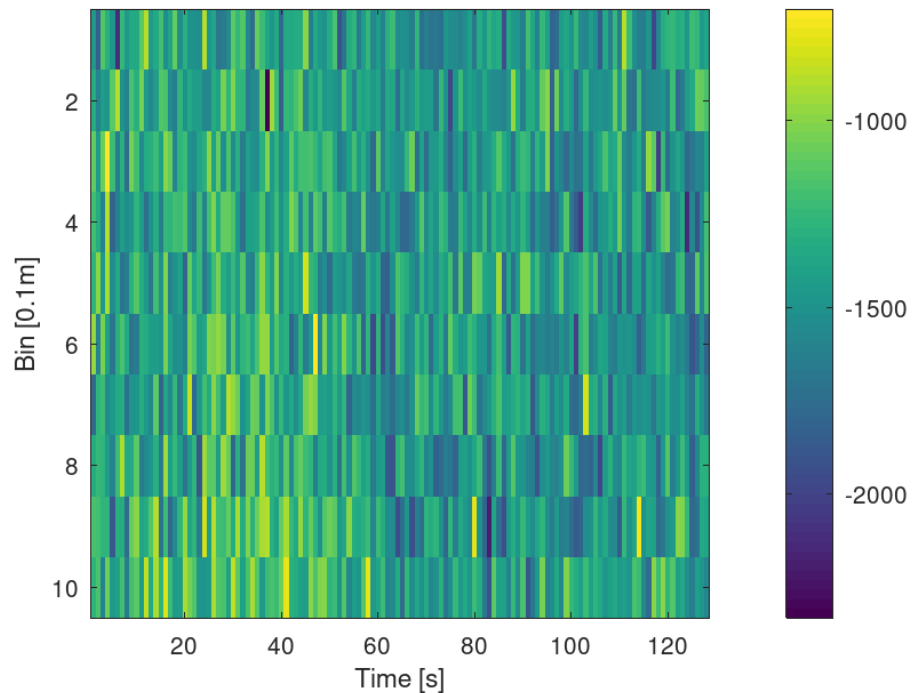
Figure A6. Waterfall plot of filtered inflow x–velocity for Aquadopp 2 in mm/s. Bin size is 0.1 m.

References

1. Gaurier, B.; Germain, G.; Facq, J.; Johnstone, C.; Grant, A.; Day, A.; Nixon, E.; de Felice, F.; Constanzo, M. Tidal energy "Round Robin" tests—Comparisons between towing tank and circulating tank results. *Int. J. Mar. Energy* **2015**, *12*, 87–109. [CrossRef]
2. Martinez, R.; Gaurier, B.; Ordonez-Sanchez, S.; Facq, J.V.; Germain, G.; Johnstone, C.; Santic, I.; Salvatore, F.; Davey, T.; Old, C.; et al. Tidal Energy Round Robin Tests: A Comparison of Flow Measurements and Turbine Loading. *J. Mar. Sci. Eng.* **2021**, *9*, 425. [CrossRef]
3. Gaurier, B.; Ordonez-Sanchez, S.; Facq, J.V.; Germain, G.; Johnstone, C.; Martinez, R.; Salvatore, F.; Santic, I.; Davey, T.; Old, C.; et al. MaRINET2 Tidal Energy Round Robin Tests—Performance Comparison of a Horizontal Axis Turbine Subjected to Combined Wave and Current Conditions. *J. Mar. Sci. Eng.* **2020**, *8*, 463. [CrossRef]
4. Atcheson, M.; MacKinnon, P.; Elsaesser, B. A large scale model experimental study of a tidal turbine in uniform steady flow. *Ocean Eng.* **2015**, *110*, 51–61. [CrossRef]
5. Starzmann, R.; Baldus, M.; Groh, E.; Hirsch, N.; Lange, N.A.; Scholl, S. Full-Scale Testing of a Tidal Energy Converter Using a Tug Boat. In Proceedings of the European Wave & Tidal Energy Conference, Aarlborg, Denmark, 2–5 September 2013; Volume 10.
6. Starzmann, R.; Jeffcoate, P.; Scholl, S.; Bischoff, S.; Elsaesser, B. Field testing a full-scale tidal turbine. In Proceedings of the 11th European Wave and Tidal Energy Conference, Nantes, France, 6–11 September 2015; pp. 6–11.
7. Cavagnaro, R.J.; Polagye, B. Field performance assessment of a hydrokinetic turbine. *Int. J. Mar. Energy* **2016**, *14*, 125–142. [CrossRef]
8. Kirke, B. Tests on ducted and bare helical and straight blade Darrieus hydrokinetic turbines. *Renew. Energy* **2011**, *36*, 3013–3022. [CrossRef]
9. Kinsey, T.; Dumas, G.; Lalande, G.; Ruel, J.; Méhut, A.; Viarouge, P.; Lemay, J.; Jean, Y. Prototype testing of a hydrokinetic turbine based on oscillating hydrofoils. *Renew. Energy* **2011**, *36*, 1710–1718. [CrossRef]
10. Frost, C.; Benson, I.; Jeffcoate, P.; Elsäßer, B.; Whittaker, T. The effect of control strategy on tidal stream turbine performance in laboratory and field experiments. *Energies* **2018**, *11*. 1533. [CrossRef]
11. Frost, C.; Benson, I.; Elsäßer, B.; Starzmann, R.; Whittaker, T. Mitigating Uncertainty in Tidal Turbine Performance Characteristics from Experimental Testing. In Proceedings of the European Wave & Tidal Energy Conference, Cork, Ireland, 27 August–1 September 2017; Volume 27.
12. Ruopp, A.; Daus, P.; Biskup, F.; Riedelbauch, S. Performance prediction of a tidal in-stream current energy converter and site assessment next to Jindo, South Korea. *J. Renew. Sustain. Energy* **2015**, *7*, 061707. [CrossRef]
13. Torrens-Spence, H.; Schmitt, P.; Frost, C.; Benson, I.; MacKinnon, P.; Whittaker, T. Assessment of Flow Characteristics at Two Locations in an Energetic Tidal Channel. In Proceedings of the Twelfth European Wave and Tidal Energy Conference, Cork, Ireland, 27 August–1 September 2017.

14. Bahaj, A.; Molland, A.; Chaplin, J.; Batten, W. Power and thrust measurements of marine current turbines under various hydrodynamic flow conditions in a cavitation tunnel and a towing tank. *Renew. Energy* **2007**, *32*, 407–426. [CrossRef]

15. Fu, S.; Ordonez-Sanchez, S.; Martinez, R.; Johnstone, C.; Allmark, M.; O'Doherty, T. Using Blade Element Momentum Theory to Predict the Effect of Wave-Current Interactions on the Performance of Tidal Stream Turbines. *Int. Mar. Energy J.* **2021**, *4*, 25–36. [CrossRef]

16. Mori, N.; Suzuki, T.; Kakuno, S. Experimental study of air bubbles and turbulence characteristics in the surf zone. *J. Geophys. Res.* **2007**, *112*. [CrossRef]

17. Allmark, M.; Ellis, R.; Lloyd, C.; Ordonez-Sanchez, S.; Johannesen, K.; Byrne, C.; Johnstone, C.; O'Doherty, T.; Mason-Jones, A. The development, design and characterisation of a scale model Horizontal Axis Tidal Turbine for dynamic load quantification. *Renew. Energy* **2020**, *156*, 913–930. [CrossRef]

18. Ellis, R.; Allmark, M.; O'Doherty, T.; Mason-Jones, A.; Ordonez-Sanchez, S.; Johannesen, K.; Johnstone, C. Design process for a scale horizontal axis tidal turbine blade. In Proceedings of the 4th Asian Wave and Tidal Energy Conference, AWTEC 2018, Taipei, Taiwan, 9–13 September 2018.

19. Nevalainen, T.; Johnstone, C.; Grant, A. A sensitivity analysis on tidal stream turbine loads caused by operational, geometric design and inflow parameters. *Int. J. Mar. Energy* **2016**, *16*, 51–64. [CrossRef]

20. Ordonez-Sanchez, S.; Ellis, R.; Porter, K.; Allmark, M.; O'Doherty, T.; Mason-Jones, A.; Johnstone, C. Numerical models to predict the performance of tidal stream turbines working under off-design conditions. *Ocean Eng.* **2019**, *181*, 198–211. [CrossRef]

21. Galloway, P.W.; Myers, L.E.; Bahaj, A.S. Quantifying wave and yaw effects on a scale tidal stream turbine. *Renew. Energy* **2014**, *63*, 297–307. [CrossRef]